Low-threshold, single-mode, and linearly polarized lasing from all organic quasicrystal microcavity

ZONGDAI LIU,[1] RUI CHEN,[1] YANJUN LIU,[1] XINHAI ZHANG, [1] XIAOWEI SUN,[1] WENBIN HUANG,[2,3,4] AND DAN LUO[1,5]

[1]*Department of Electrical & Electronic Engineering, Southern University of Science and Technology, Xueyuan Road 1088, Shenzhen, Guangdong 518055, China*
[2]*College of Physics, Optoelectronics and Energy & Collaborative Innovation Center of Suzhou Nano Science and Technology, Soochow University, Suzhou, 215006, China*
[3]*Key Lab of Advanced Optical Manufacturing Technologies of Jiangsu Province & Key Lab of Modern Optical Technologies of Education Ministry of China, Soochow University, Suzhou, 215006, China*
[4]*wbhuang@suda.edu.cn*
[5]*luod@sustc.edu.cn*

Abstract: Organic microcavity lasers based on liquid crystals have attracted substantial attention due to their easy processing, compact volume and excellent tunable properties. However, the threshold of traditional holographic polymer dispersed liquid crystals (H-PDLCs) laser doped with dye is usually as high as several tens of μJ/pulse, which hinders its broad applications. Herein, we demonstrate a low-threshold lasing from quasicrystal based on H-PDLCs. An conjugated polymer poly (2-methoxy-5-(2'-ethyl-hexyloxy)-p-phenylenevinylene (MEH-PPV) film is coated on the inner surface of glass substrate to dramatically reduce the lasing threshold, which is 20 times lower than that of dye-doped microcavity laser. A low threshold, single-mode, linearly polarized lasing is achieved when the thickness of MEH-PPV film is optimized at 80 nm. Due to its easy fabrication, excellent performance and bio-compatibility, this compact coherent light source may be useful in lab-on-chip applications such as detection, sensing and analyzing, as well as display, optical communications, and other photonic fields.

References and links

1. H. Coles and S. Morris, "Liquid-crystal lasers," Nat. Photonics **4**(10), 676–685 (2010).
2. R. Sutherland, V. Tondiglia, L. Natarajan, S. Chandra, D. Tomlin, and T. Bunning, "Switchable orthorhombic F photonic crystals formed by holographic polymerization-induced phase separation of liquid crystal," Opt. Express **10**(20), 1074–1082 (2002).
3. V. I. Kopp, B. Fan, H. K. M. Vithana, and A. Z. Genack, "Low-threshold lasing at the edge of a photonic stop band in cholesteric liquid crystals," Opt. Lett. **23**(21), 1707–1709 (1998).
4. M. Ozaki, M. Kasano, D. Ganzke, W. Haase, and K. Yoshino, "Mirrorless lasing in a dye - doped ferroelectric liquid crystal," Adv. Mater. **14**(4), 306–309 (2002).
5. H. Takezoe, K. Kondo, A. Fukuda, and E. Kuze, "Determination of helical pitch in homeotropic cell of chiral smectic C liquid crystal using F-center laser," Jpn. J. Appl. Phys. **21**(2), L627–L629 (1982).
6. D. Luo, X. W. Sun, H. T. Dai, Y. J. Liu, H. Z. Yang, and W. Ji, "Two-directional lasing from a dye-doped two-dimensional hexagonal photonic crystal made of holographic polymer-dispersed liquid crystals," Appl. Phys. Lett. **95**(15), 2059 (2009).
7. W. Cao, A. Muñoz, P. Palffy-Muhoray, and B. Taheri, "Lasing in a three-dimensional photonic crystal of the liquid crystal blue phase II," Nat. Mater. **1**(2), 111–113 (2002).
8. D. Shechtman, I. Blech, D. Gratias, and J. W. Cahn, "Metallic phasewith long-range orientational order and no translational symmetry," Phys. Rev. Lett. **53**(20), 1951–1953 (1984).
9. S. P. Gorkhali, J. Qi, and G. P. Crawford, "Switchable quasi-crystal structures with five-, seven-, and ninefold symmetries," J. Opt. Soc. Am. B **23**(1), 149–158 (2006).
10. J. Joannopoulos, R. D. Meade, and J. Winn, *Photonic Crystals: Molding the Flow of Light* (Princeton University, 1995).

11. C. Jin, B. Cheng, B. Man, Z. Li, D. Zhang, S. Ban, and B. Sun, "Band gap and wave guiding effect in a quasiperiodic photonic crystal," Appl. Phys. Lett. **75**(13), 1848–1850 (1999).
12. Y. S. Chan, C. T. Chan, and Z. Y. Liu, "Photonic band gaps in two dimensional photonic quasicrystals," Phys. Rev. Lett. **80**(5), 956–959 (1998).
13. M. Notomi, H. Suzuki, T. Tamamura, and K. Edagawa, "Lasing action due to the two-dimensional quasiperiodicity of photonic quasicrystals with a Penrose lattice," Phys. Rev. Lett. **92**(12), 123906 (2004).
14. D. Luo, Q. G. Du, H. T. Dai, H. V. Demir, H. Z. Yang, W. Ji, and X. W. Sun, "Strongly linearly polarized low threshold lasing of all organic photonic quasicrystals," Sci. Rep. **2**(1), 627 (2012).
15. D. Luo, Y. Li, X. W. Xu, and Q. G. Du, "Lasing from organic quasicrystal fabricated by seven- and nine-beam interference," Opt. Express **24**(11), 12330–12335 (2016).
16. Z. Liu, D. Luo, Q. Du, Y. Li, and H. Dai, "Emission characteristics of lasing from all organic mirrorless quasicrystal," IEEE Photonics J. **8**(6), 1–6 (2016).
17. D. Luo, Q. G. Du, H. T. Dai, X. H. Zhang, and X. W. Sun, "Temperature effect on lasing from Penrose photonic quasicrystal," Opt. Mater. Express **4**(6), 1172–1177 (2014).
18. T. Woggon, S. Klinkhammer, and U. Lemmer, "Compact spectroscopy system based on tunable organic semiconductor lasers," Appl. Phys. B **99**(1), 47–51 (2010).
19. Y. Yang, G. A. Turnbull, and I. D. W. Samuel, "Sensitive explosive vapor detection with polyfluorene lasers," Adv. Funct. Mater. **20**(13), 2093–2097 (2010).
20. J. Clark and G. Lanzani, "Organic photonics for communications," Nat. Photonics **4** (7), 438 –446 (2010).
21. M. Uchimura, Y. Watanabe, F. Araoka, J. Watanabe, H. Takezoe, and G. Konishi, "Development of laser dyes to realize low threshold in dye-doped cholesteric liquid crystal lasers," Adv. Mater. **22**(40), 4473–4478 (2010).
22. K. Kim, S. T. Hur, S. Kim, S. Y. Jo, B. R. Lee, M. H. Song, and S. W. Choi, "A well-aligned simple cubic blue phase for a liquid crystal laser," J. Mater. Chem. C Mater. Opt. Electron. Devices **3**(21), 5383–5388 (2015).
23. L. Wang, Y. Wan, L. Shi, H. Zhong, and L. Deng, "Electrically controllable plasmonic enhanced coherent random lasing from dye-doped nematic liquid crystals containing Au nanoparticles," Opt. Express **24**(16), 17593–17602 (2016).
24. E. Perju, E. Paslaru, and L. Marin, "Polymer-dispersed liquid crystal composites for bio-applications: thermotropic, surface and optical properties," Liq. Cryst. **42**(3), 370–382 (2015).
25. D. Ailincai, C. Farcau, E. Paslaru, and L. Marin, "PDLC composites based on polyvinyl boric acid matrix - a promising pathway towards biomedical engineering," Liq. Cryst. **43**(13–15), 1973–1985 (2016).
26. S. J. Woltman, G. D. Jay, and G. P. Crawford, "Liquid-crystal materials find a new order in biomedical applications," Nat. Mater. **6**(12), 929–938 (2007).
27. Y. J. Liu, X. W. Sun, P. Shum, and X. J. Yin, "Tunable fly's-eye lens made of patterned polymer-dispersed liquid crystal," Opt. Express **14**(12), 5634–5640 (2006).
28. W. Huang, Z. Diao, Y. Liu, Z. Peng, C. Yang, J. Ma, and L. Xuan, "Distributed feedback polymer laser with an external feedback structure fabricated by holographic polymerization technique," Org. Electron. **13**(11), 2307–2311 (2012).
29. W. Huang, L. Chen, and L. Xuan, "Efficient laser emission from organic semiconductor activated holographic polymer dispersed liquid crystal transmission gratings," RSC Adv. **4**(73), 38606–38613 (2014).
30. M. Liu, Y. Liu, G. Zhang, Z. Peng, D. Li, J. Ma, and L. Xuan, "Organic holographic polymer dispersed liquid crystal distributed feedback laser from different diffraction orders," J. Phys. D Appl. Phys. **49**(46), 465102 (2016).
31. M. Liu, Y. Liu, G. Zhang, L. Liu, Z. Diao, C. Yang, Z. Peng, L. Yao, J. Ma, and L. Xuan, "Improving the conversion efficiency of an organic distributed feedback laser by varying solvents of the laser gain layer," Liq. Cryst. **43**(3), 417–426 (2016).

1. Introduction

Organic microcavity lasers based on liquid crystals (LCs) have attracted substantial attention over past decades owing to their easy processing, compact volume and excellent tunable properties [1,2]. Several kinds of liquid crystal laser have been reported such as cholesteric liquid crystals [3], ferroelectric liquid crystals [4], smectic liquid crystals [5], polymer dispersed liquid crystals [6], and blue phase liquid crystals [7]. Two-dimensional (2D) quasicrystals with aperiodic structures have been fabricated by polymer dispersed liquid crystals (PDLCs) which exhibit advantages of tunability, compactness and easy processing. Quasicrystal is an intermediate state between the crystalline texture and the amorphous one [8]. The atomic positions are ordered with rotational symmetries, e.g. five-, seven-, nine-, and twelve-, which are not found in crystals [9]. Similar to photonic crystals, photonic quasicrystals possess photonic band gap as well [10–13].

Recently, lasing from dye-doped quasicrystal has been reported and the lasing generation mechanism could be attributed to the bandgap effect [14,15]. In our previous studies, we have reported quasicrystal microcavity lasers with linear polarization as well as temperature

tunability [16,17]. Features of mirrorless laser from quasicrystal based on H-PDLC include directional light source, simple fabrication process, low cost and tunability. This kind of laser can be used in many potential practical applications, e.g. high-resolution spectroscopic analyzing [18], high sensitive vapor sensors [19], and ultra-fast switches in optical data communication [20]. However, for quasicrystal microcavity lasers based on dye-doped H-PDLC (27 μJ/pulse) [15], the pump threshold is relatively high, compared to dye-doped cholesteric liquid crystal lasers (23 nJ/pulse) [21], blue phase liquid crystal lasers (3.3 μJ/pulse) [22], and dye-doped nematic liquid crystal (6.60 μJ/pulse) [23], due to the relatively low refractive index contrast between liquid crystal and polymer, thus prevents its broadly applications. If the threshold can be reduced, miniature pulse lasers or even pulse light emitting diodes (LEDs) can be used to replace pulse laser as the pumping source, making it easier to integrate into a chip. Additionally, the low threshold is critical to the long lifetime of organic laser.

In this paper, we demonstrate low threshold lasing from all-organic quasicrystals fabricated by multi-beam interference. A thin film layer of conjugated polymer poly (2-methoxy-5-(2'-ethyl-hexyloxy)-p-phenylenevinylene (MEH-PPV) is coated on the inner surface of one glass substrate as the optical gain medium. Compared with the traditional microcavity lasers based on dye-doped quasicrystals, the pump threshold of MHE-PPV film coated quasicrystal microcavity is dramatically reduced by 20 times. The thickness of MEH-PPV film plays a crucial role in lasing characteristics, which has also been demonstrated and optimized, resulting in a low threshold, single mode, and linearly polarized lasing. Due to its easy fabrication, excellent performance and bio-compatibility [24–27], this compact coherent light source may be useful in lab-on-chip applications such as detection, sensing and analyzing, and many other photonic fields.

2. Experiment

In our experiment, the sample mixture was consisted of 65 wt% monomer, trimethylolpropane triacrylate (TMPTA), 8 wt% cross-linking monomer, N-vinylpyrrollidone (NVP), 0.8 wt% photoinitiator, Rose Bengal (RB), and 1 wt% coinitiator, N-phenylglycine (NPG), all from Sigma-Aldrich, and 24 wt% liquid crystal, E7 ($n_o = 1.5216$ and $n_e = 1.7462$) from Merck. To fabricate the LC cell, two pieces of glass substrate were cleaned by acetone, ethanol, and deionized water in ultrasonic environment for 30 minutes in sequence and dried by nitrogen. Then, the solution of organic semiconductor poly (2-methoxy-5-(2'-ethyl-hexyloxy)-p-phenylenevinylene, MEH-PPV) (Jilin OLED Material Co., Ltd) in toluene (5 mg/mL) was spin-coated (2000-4000 rpm; 30 s) on the surface of one glass substrate. The thickness of MEH-PPV film was between 60 nm and 100 nm, depending on the rotation speed. After that, LC cell was assembled by an empty glass substrate and a glass substrate coated with MEH-PPV. The thickness of cell was 20 μm. The LC/monomer mixture was mechanically stirred for several hours at temperature of 60 °C, and then injected into the cell.

Different from laser dye, MEH-PPV is a kind of organic semiconductor, which possesses large cross-section for stimulated emission and serves as quasi-four-level laser material where the population inversion condition can be achieved easily. MEH-PPV films have already been demonstrated as good lasing materials and they can be simply deposited from solution by spin-coating [21-22]. In this experiment, MEH-PPV was chosen to be gain medium by forming a thin film through spin-coating. Toluene solution with 5 mg/mL concentration of MEH-PPV was prepared and spin-coated on the glass substrate.

The quasicrystal nanostructure was fabricated by a single-step exposure with a specially designed prism. The prism was fabricated by fused silica with a refractive index of 1.46, where the bottom plane was an equilateral heptagon and the angle between the side plane and bottom plane was $\Phi = 60°$, as shown in Fig. 1(a). A linearly polarized Ar$^+$ laser (Coherent, I-306C, 488 nm) beam was collimated and impinged on the prism and then split into 7 beams with wave vectors of k_n ($n = 1 \sim 7$). The wave vectors of seven beams can be expressed as:

$$k_n = k\left(-\cos\frac{2(n-1)\pi}{7}\sin\theta, -\sin\frac{2(n-1)\pi}{7}\sin\theta, -\cos\theta\right), \tag{1}$$

where n is an integer from 1 to 7, $k = 2\pi n_{eff}/\lambda$ is the unit wave vector, λ is the writing wavelength in the air, n_{eff} is the effective refractive index of the recording material, and θ represents the angle between the beam and vertical z axis. Here, we have $\theta_1 \sim \theta_7 = \theta = 23.6°$, $\lambda = 488$ nm, and $n_{eff} = 1.524$.

The interference pattern was formed at the bottom of prism where the LC cell with sample mixture was placed to record the pattern. The intensity of interference pattern can be given by:

$$I(r) = \Re\left(\sum_{l,m=1}^{7} E_l \cdot E_m \exp[i(k_l - k_m)\cdot r]\right), \tag{2}$$

where l and m are integers from 1 to 7, E is the electric field, $r = (x, y, z)$ is the position vector, and $\Re[...]$ denotes the real part of the argument. The exposure intensity of each beam was ~ 9 mW/cm^2 and the exposure time was 150 s. Due to the light induced polymerization and phase separation between LC and polymer, the bright regions (high intensity) and dark regions (low intensity) were composed of cured polymers and LC, respectively. The schematic configuration of formed quasicrystal structure with MEH-PPV film in LC cell was shown in Fig. 1(b).
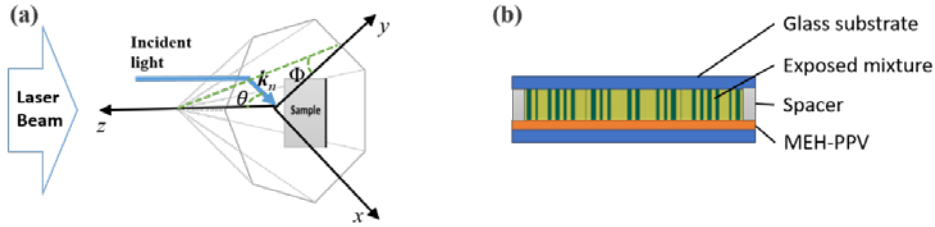

Fig. 1. The fabrication process of the cell. (a) Optical setup used for seven-beam interference. k_n is the wave vector, θ represents the angle between the beam and vertical z axis, Φ represents the angle between the side and bottom plane. A laser beam was split into seven beams through the prism and interfered with each other. The interfered pattern was recorded by the cell filled with LC/monomer mixture. (b) Quasicrystal structure formed.

In lasing generation part, a Q-switched Nd:yttrium-aluminum-garnet (Nd:YAG) pulsed laser (Quantel, Q-smart 450, 532 nm) was expanded and collimated by a beam expander. After that, the pump beam was focused by a cylindrical lens, and then impinged on the surface of the sample in the shape of a narrow line, as shown in Fig. 2(b). The pulse duration and repetition rate of the pump laser was 10 ns and 10 Hz, respectively. A beam splitter and a photodetector (as energy meter) were used to monitor the energy of each pump pulse. The output lasing was collected by a spectrometer with resolution of 0.05 nm (USB2000 + , Ocean optics).
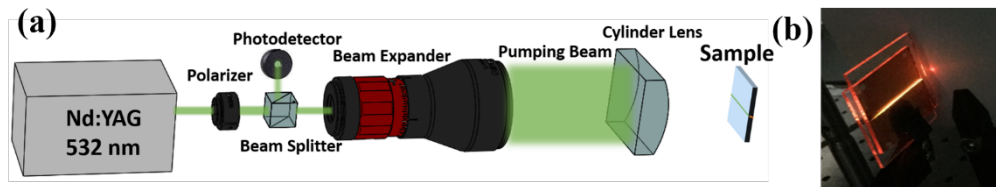

Fig. 2. (a) The optical setup of lasing generation. A Q-switched frequency-doubled Nd:YAG pulsed laser with 532 nm lasing was used to pump the quasicrystal structure. The pump beam was focused by a cylindrical lens, and then impinged on the surface of the sample in the shape of a narrow line. (b) The photo of generated lasing spot.

3. Results and discussion

Figure 3(a) shows simulated structure of aperiodic quasicrystal formed by 7-beam interference. The green- and yellow-area represents relatively high- and low-intensity region, corresponding to polymer-rich and LC-rich region, respectively. The output lasing was generated along the direction of OO'. The surface morphology was observed by atomic force microscopy (AFM) after removing LCs in ethanol, as shown in Fig. 3(b). The circle indicated the polymer regions with 2N (N = 7) symmetry locations that was consistent with the simulated pattern.
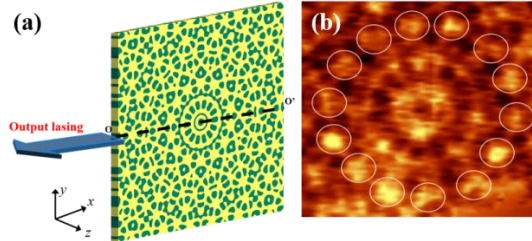

Fig. 3. (a) The simulated pattern of aperiodic quasicrystal formed by 7-beam interference. After light induced polymerization, phase separation of polymer and LC occurred. The green- and yellow-area represents relatively high- and low-intensity region, corresponding to polymer-rich and LC-rich region, respectively. Pumping line (OO') is at the center of quasicrystal structure. (b) The AFM image of surface of seven-beam interference pattern. White region in the circle represents polymer region with 2N (N = 7) symmetry locations.
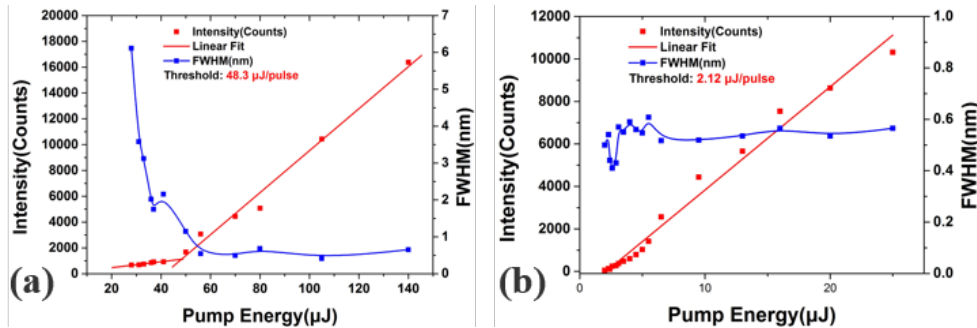

Fig. 4. The output intensity and line width verse pumping energy. (a) Lasing peak at 632 nm for DCM doped quasicrystal, where the threshold was 48.0 µJ/pulse. (b) Lasing peak at 629 nm for MEH-PPV film coated quasicrystal, where the threshold was dramatically reduced to 2.12 µJ/pulse.

For comparison purpose, a quasicrystal sample doped with DCM was prepared, where no MEH-PPV film was used in this sample. The laser dye of DCM was chosen here because of similar photoluminescence spectral to MEH-PPV. The dependence of output energy and line width of lasing on the pump energy for laser dye DCM and MEH-PPV is shown in Fig. 4(a) and 4(b), respectively. The thresholds of lasing at 632 nm in DCM case and at 629 nm in MEH-PPV case were found to be 48.3 µJ/pulse and 2.12 µJ/pulse, respectively, keeping other parameters unchanged. It can be seen that the threshold for MEH-PPV case was dramatically reduced more than 20 times while keeping full width at half maxima (FWHM) almost unchanged, comparing to 12.5~16.7 times reduction of threshold in previously reported transmittance grating cases [28–31]. One possible explanation might be due to the high photoluminescence quantum yield (PLQY) of MEH-PPV comparing to laser dye DCM. It was well known that the dye material like DCM suffered from concentration quench, which resulted in low solubility of DCM in H-PDLCs and was directly associated with the low PLQY. In contrast, the MEH-PPV film possessed higher PLQY thus leaded to the lower

threshold. Furthermore, for dye-doped case, larger scattering loss occurs due to relatively larger difference of refractive index between liquid crystal and polymer, while photons experience in homogenous MEH-PPV film for MEH-PPV case. Therefore, scattering loss can be alleviated and better performance can be obtained by applying MEH-PPV film as active layer.

Besides pump threshold, the polarization of output lasing was also an important parameter. In our experiment, a polarizer was placed between the sample and the spectrometer to measure the polarization property of output lasing beam. The experimental data showed that an excellent linearly polarized lasing with calculated polarization extinction ratio of 10.2 was obtained from MEH-PPV film coated quasicrystal. The relationship of intensity of output lasing at different polarization directions was shown in Fig. 5(a), where the experimental data were presented by the black dots and the fitted since curve was plotted in red. Here, the R^2 stands for the goodness of fitting, and $R^2 = 0.990$ means that the measured data fits sine curve quite well. The possible explanation is following: the LC droplets in H-PDLCs exist in a form of bipolar configuration, which possess a director, as shown in Fig. 5(b). Along z direction, the refractive index of LC molecules is the ordinary refractive index of $n_o = 1.5216$, which is almost the same to the polymer index of $n_p = 1.5220$. Therefore, for light with polarization direction along z axis (corresponding to the angle of 90° in Fig. 5(a)), it will experience very small index contrast, leading to non-lasing signal. In contrast, for light with polarization direction along y axis (corresponding to 0° or 180°), it will experience relative large index contrast due to the difference of extraordinary index of liquid crystal droplets (n_e) and n_p of polymer. The relatively larger index contrast, extraordinary refractive index n_e (1.7462) and n_p, is experienced in y direction. Therefore lasing was obtained with polarization.
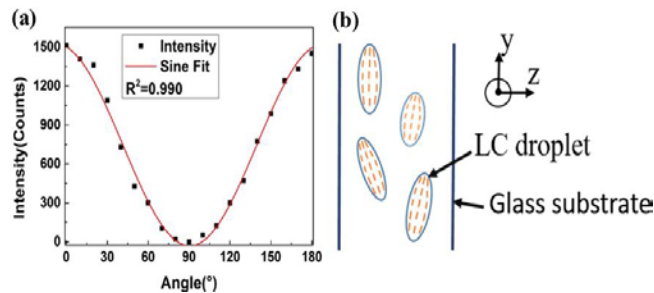

Fig. 5. (a) Lasing at different polarization direction from 0° to 180°. Black dots present the measured data and the red line is the fitted sine curve. (b) Schematic of LC droplets with bipolar configuration, where the directors in H-PDLC structure is random oriented in *y-z* plane.

To understand the effect of MEH-PPV film thickness on lasing property, three samples coated with different thickness of MEH-PPV films, such as 60 nm, 80 nm and 100 nm, were prepared and measured at pump energy of 14 μJ/pulse, as shown in Figs. 6(a)-6(c). For 60 nm thickness film (Fig. 6(a)), a lasing with peak wavelength of 632 nm that is accompanied by several sub-peaks, is achieved in the spectrum, indicating multi-mode lasing. The threshold energy was 5.94 μJ/pulse. In contrast, a single-mode lasing with a single peak of 629.68 nm was generated for 80 nm thickness film, where the threshold energy is 2.12 μJ/pulse, as shown in Fig. 6(b). When the thickness is further increased to 100 nm (Fig. 6(c)), there is even no obviously lasing emission. The optimization thick of coated MEH-PPV film seems achieved at thickness of 80 nm. For MEH-PPV film with small thickness such as 60 nm, the generated lasing mode and threshold were influenced by the volume of film, which was treated as a core of waveguide between the H-PDLC and glass substrate. The evanescent wave in waveguide (MEH-PPV film) will prefer to leak instead of being constrained. Therefore, the oscillation feedback in quasicrystal microcavity was weakened, leading to higher threshold energy. For MEH-PPV film with large thickness such as 100 nm, most of

light was bounded in the film, which limit the lasing oscillation in the quasicrystal microcavity. Therefore, the thickness of film should be chosen properly to generate lasing with sufficient amplification in quasicrystal microcavity. In our experiment, the proper thickness of MEH-PPV film was found to be 80 nm and the corresponding threshold was the lowest, and the lasing mode was the single-mode.
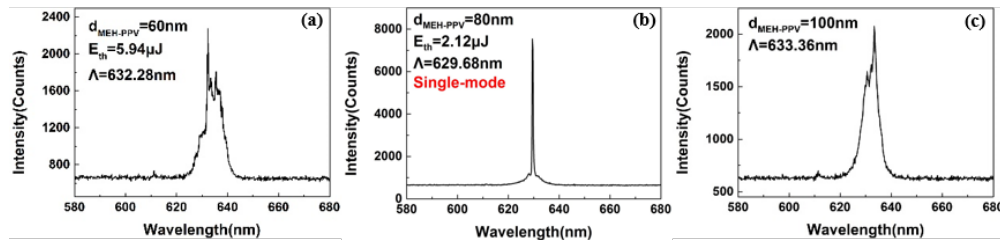

Fig. 6. Lasing emission spectra with different thickness of MEH-PPV films at 14 μJ/pulse. (a) For 60 nm thickness film, the peak is at 632 nm and the threshold is 5.94 μJ/pulse. (b) For 80 nm thickness film, the peak is at 629 nm and the threshold is 2.12 μJ/pulse. The lasing is operated at single-mode. (c) For 100 nm thickness film, the peak is at 633 nm, and no lasing is achieved.

4. Conclusion

In summary, we demonstrated low-threshold, single-mode and polarized lasing from quasicrystal microcavity based on seven-beam interference H-PDLCs. In order to reduce lasing threshold, an 80 nm thickness of MEH-PPV film was spin-coated on the surface of one substrate. Comparing to lasing from traditional dye doped quasicrystal microcavity, more than 20 times reduction of threshold has been achieved. The effect of MEH-PPV film thickness on lasing threshold, mode property and polarization characteristic has also been investigated, where an optimized thickness is experimentally obtained. We found that the high refractive-index MEH-PPV layer not only worked as an independent active layer for optical gain, but also played as the waveguide core layer for efficient mode confinement. Besides low threshold, the lasing also can be operated in single mode with excellent linear polarization, which is quite useful in many photonic and optics applications such as displays, optical communications, holography, and coherent light source.

Funding